M&C 2017 - International Conference on Mathematics & Computational Methods Applied to Nuclear Science & Engineering, Jeju, Korea, April 16-20, 2017, on USB (2017)

Performance Assessment of Cost-Optimized Variance Reduction Parameters in Radiation Shielding Scenarios

Joel A. Kulesza,[1,2] Clell J. Solomon,[2] Brian C. Kiedrowski,[1] Edward W. Larsen[1]

[1]*Department of Nuclear Engineering & Radiological Sciences, University of Michigan*
2355 Bonisteel Blvd., Ann Arbor, MI, 48109
[2]*Monte Carlo Methods, Codes, and Applications Group, Los Alamos National Laboratory*
P.O. Box 1663, Los Alamos, NM, 87545
jkulesza@umich.edu, csolomon@lanl.gov, bckiedro@umich.edu, edlarsen@umich.edu

Abstract - *This paper describes recent work on the Cost-Optimized Variance Reduction Technique (COVRT) software that is used to automatically and deterministically generate cost-optimized variance-reduction (VR) parameters for use in Monte Carlo analyses. During generation, cost optimization modifies VR parameters to efficiently reduce problem variance by considering the computational expense of each operation associated with a given variance reduction technique. In this work, the software is first modified to consider only weight-independent VR techniques (giving a computational savings by removing weight from the phase space considered) or weight-dependent (which can include weight-independent) techniques. Using only weight-independent techniques, COVRT calculations are an order of magnitude faster and require two orders of magnitude less memory than corresponding weight-dependent calculations. Once applied to Monte Carlo calculations using MCNP and with figure of merit as the measure, optimized weight-independent VR techniques are no less effective than, and up to* 2× *as effective as, optimized weight-dependent techniques. Compared to other software that does not attempt to optimize VR parameters such as ADVANTG, the COVRT-generated parameters are 1.2–5× as effective once applied in MCNP. Moreover, comparing COVRT and ADVANTG demonstrates a significant time penalty (up to five orders of magnitude for comparable calculations) for COVRT during the deterministic calculations but also a significant time savings (one to two orders of magnitude) during the Monte Carlo calculation.*

I. INTRODUCTION

This paper discusses the application of automatically generated, cost-optimized, variance-reduction (VR) parameters to several two-dimensional (2D) MCNP® calculations. During generation, cost optimization modifies variance reduction parameters to efficiently reduce problem variance by considering the computational expense of each operation associated with a given VR technique. Variance-reduction parameters are generated using the Cost-Optimized Variance Reduction Technique (COVRT) software [1] that performs a series of deterministic calculations to solve the history-score-moment and future-time equations (see Sec. II. and [1, 2]) and then iteratively optimizes the solutions. When COVRT was developed, it was designed to operate in a weight-dependent mode; i.e., to perform a discrete ordinates solve over discretized space, angle, energy, *and* weight. Since then, COVRT has been modified to perform both weight-dependent and weight-independent calculations. The motivation for this was to remove the finely discretized weight mesh from the calculation to reduce the computational burden. However, this introduces the limitation that COVRT, when running a weight-independent calculation, can only optimize parameters for techniques that modify particle weight but are not played depending on it (e.g., cell-based importances and implicit capture).

Section II presents an overview of the solution methodology. Section III provides a description of the calculations used to assess the effect of the weight-dependent and weight-independent VR parameters on the Monte Carlo transport. Section IV gives comparisons with prior results [1] (Sec. IV.1) and against ADVANTG [3] (Sec. IV.2). This paper shows that weight-independent COVRT calculations yield mean values consistent with prior weight-dependent calculations, are much faster to execute, and can lead to more efficient MCNP calculations than comparable calculations using VR parameters generated with a weight-dependent COVRT calculation. In addition, COVRT is capable of producing more efficient MCNP calculations than ADVANTG using default behavior. Finally, planned extensions to the COVRT methodology are briefly described.

II. METHODOLOGY

The methodology implemented in COVRT involves deterministically solving the history-score-moment equations, originally developed in [4] and then extended in [1, 2]. These equations are used to calculate the population mean and variance of Monte Carlo transport problems. The future-time equations developed in [1, 2] predict the time / computational cost necessary to calculate a single Monte Carlo his-

tory given a set of VR techniques. By finding a set of VR techniques that minimizes the product of the solution of both sets of equations, those VR parameters are expected to maximize the traditional MCNP figure of merit (FOM), proportional to $\sigma^{-2}T^{-1}$, where σ is the Monte Carlo tally standard deviation and T is the Monte Carlo calculation time. Note that throughout this paper final COVRT-calculated values are shown with tildes (e.g., $\widetilde{\sigma}$) and MCNP-calculated values are shown unaccented.

More details regarding the development and extension of the history-score-moment and future-time equations are available in the aforementioned references, but briefly consider the traditional time-independent radiation transport phase space $\boldsymbol{R} = (\boldsymbol{x}, \boldsymbol{\Omega}, E)$, where $\boldsymbol{x}$ represents position, $\boldsymbol{\Omega}$ represents direction of flight, and E represents energy, which can be augmented with Monte Carlo particle weight, w, to form $\boldsymbol{P} = (\boldsymbol{x}, \boldsymbol{\Omega}, E, w) = (\boldsymbol{R}, w)$. Next, a series of scoring functions, transport kernels, and weight-modifying functions are defined to describe all the ways that a particle can contribute a score in ds about s in its next event, how a particle can transition from one region of phase space to another, and any associated weight changes with that phase-space transition, respectively. Finally, the history-score distribution function $\psi(\boldsymbol{P}, s)\, ds$ is defined which gives the probability that a particle at $\boldsymbol{P}$ and all its progeny will score in ds about s. Thus, the m moments of the history-score distribution are

$$M_m(\boldsymbol{P}) \equiv \int_{-\infty}^{\infty} s^m \psi(\boldsymbol{P}, s)\, ds. \tag{1}$$

Considering only weight-independent VR techniques (e.g., cell-based importances, implicit capture), one can separate w from $\boldsymbol{P}$ to obtain

$$M_m(\boldsymbol{R}, w) = w^m M_m(\boldsymbol{R}, w = 1). \tag{2}$$

This separation removes the necessity of treating weight in the discrete ordinates calculation explicitly (but, again, removes the opportunity to consider weight-dependent VR techniques such as weight windows and/or weight cutoff). For both the first and second moments, integro-differential transport equations are formed and solved. The solutions for M_m, $m = 1, 2$ are then used to find the corresponding tally (or detector) responses

$$\widetilde{D}_m = \int_{\boldsymbol{P}} M_m(\boldsymbol{P})\, S(\boldsymbol{P})\, dP,\ m = 1, 2 \tag{3}$$

where $S(\boldsymbol{P})$ is the physical source term. This is comparable to solving for statistical moments of the adjoint flux and using them to determine the associated detector response statistical moments. Note that lower moments generally act as a source for higher moments. As such, solving these equations requires solving the first moment and then progressively solving higher moments. Using these responses, the population variance is deterministically calculated as

$$\widetilde{\sigma}^2 = \widetilde{D}_2 - \widetilde{D}_1^2. \tag{4}$$

In addition, the expected computational time required for a Monte Carlo calculation to process a single history, $\widetilde{\tau}$, can be deterministically estimated as the accumulation of the time required to process various events (source emission, collision, banking, surface crossing, nuclear data lookup, etc.) that the history is expected to undergo from beginning to end. The time required for individual events is estimated by profiling a short Monte Carlo calculation representative of the problem at hand. The calculation is run with all VR capabilities enabled that are planned for optimization in COVRT and is analyzed with Valgrind's Callgrind utility [5, 6]. Callgrind provides the number of calls to routines corresponding to the various events (source emission: `startp`, collision: `colidn`, banking: `bankit`, etc.) and the associated number of instructions processed. Using the total run time, the total number of instructions performed, and by segregating the routines of interest, one can estimate the time necessary for each routine's call (with the assumption that all instructions are approximately of equal duration). The time per call is generally 10^{-7}–10^{-8} minutes as shown in [2]. Because relative differences in routine times are of primary interest, profiling does not need to happen regularly. Instead, it should be performed periodically as significantly different problems are analyzed and/or when the Monte Carlo program flow changes to ensure that new relative (in)efficiencies are captured appropriately.

Next, the future-time distribution, $\Upsilon(\boldsymbol{P}, \tau)\, d\tau$, is derived which gives the probability that a particle at $\boldsymbol{P}$ requires a computation time in $d\tau$ about τ to process. The future-time distribution is similar to the history-score-moment equation except that rather than contributed score for a particular event it uses contributed time for each event based on the previously described time estimates. The expected future time of a particle at $\boldsymbol{P}$ is then calculated as

$$\overline{\tau}(\boldsymbol{P}) = \int_0^{\infty} \tau \Upsilon(\boldsymbol{P}, \tau)\, d\tau. \tag{5}$$

The expected future time of a particle is then calculated similar to the tally responses as

$$\widetilde{\tau} = \int_{\boldsymbol{P}} \overline{\tau}(\boldsymbol{P})\, S(\boldsymbol{P})\, dP \tag{6}$$

where this equation is simplified from [2] to include both the initial source processing time and the time from subsequent events.

Finally, for a given set of VR techniques, $\{V\}$, the expected cost is

$$\widetilde{C}(\{V\}) = \widetilde{\sigma}^2(\{V\})\, \widetilde{\tau}(\{V\}), \tag{7}$$

which is inversely proportional to a traditional Monte Carlo FOM. Thus, minimizing the expected cost by selecting an appropriate set of VR techniques maximizes the FOM. In COVRT, optimization is performed with the gradient descent method using variously perturbed VR parameters.

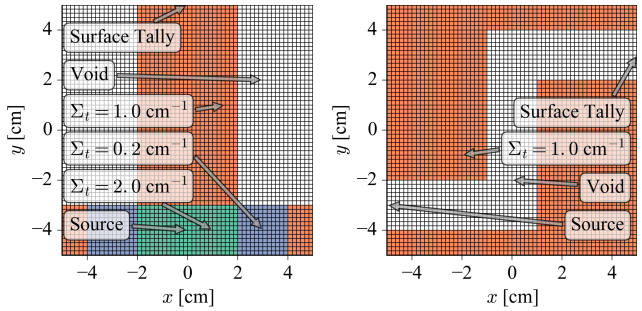

(a) Tophat, $c = 0.8$ (b) Three-Legged Duct, $c = 0.8$

Figure 1: Tophat & Three-Legged Duct Geometries

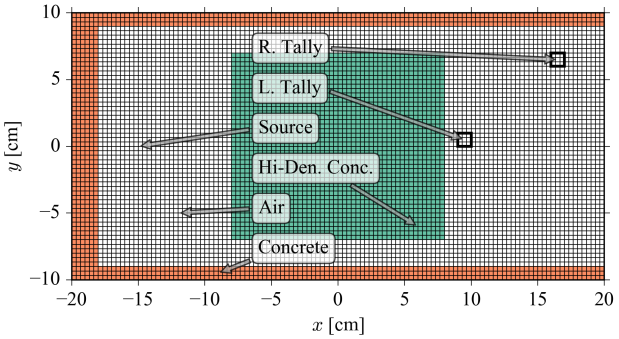

Figure 2: Mini2Room Geometry

III. DESCRIPTION OF TEST PROBLEMS

Three test problems are used to measure the effectiveness of both the weight-dependent and weight-independent implementations of the methodology. Three-dimensional (3D) calculations for anything other than exceedingly small problems with coarse angular discretization require 100s of gigabytes of computer memory for weight-dependent calculations because of the addition of weight (i.e., a weight mesh discretized with 100s–1000s of cells) to the problem domain. As such, all test problems described herein are 2D.

Of the test problems, the Tophat & Three-Legged Duct test problems are from [1]. The Mini2Room problem is a scaled-down version of a test problem similar to that described for nonproliferation applications [7]. Tophat and Three-Legged Duct problems are used to perform intercomparisons between COVRT's weight-dependent and weight-independent modes. The Mini2Room problem is used for comparison with ADVANTG. When images of the geometries are shown, the grid displayed represents the spatial mesh used in COVRT.

1. Tophat

The first test problem considered is "Tophat," which is a simplified version of the VR test problem described in [8] and is shown in Fig. 1a. Tophat is characterized by an isotropic volume source located in the region $-2 \le x \le 2, -5 \le y \le -3$ and a surface current tally located at $-2 \le x \le 2, y = 5$. The problem is monoenergetic. Between the source and surface tally are a variety of materials (all with isotropic scattering ratio $c = 0.8$) that allow particles to bypass a directly vertical path and instead leak out the "brim," stream through the void, and then reenter the hat just before the tally. This path is known to cause over-splitting of particles when VR is applied. Within MCNP, cells are 1 cm × 1 cm to provide sufficient cells to optimize over.

2. Three-Legged Duct

Next, the "Three-Legged Duct" problem is characterized by an isotropic surface source at $x = -5, -4 \le y \le -2$ and a surface current tally located at $x = 5, 2 \le y \le 4$ and is shown in Fig. 1b. The problem is monoenergetic. All non-void material has isotropic scattering ratio $c = 0.8$. Similar to Tophat, this test problem is known to oversplit particles because of the ability for particles to easily move from less-important to more-important phase space (i.e., from the shield through the duct and back into the shield). Furthermore, as Monte Carlo particles traverse the problem they can take a tortuous path with many weight-reducing collisions, or, a somewhat direct path through the duct with few collisions to reach the tally region. This leads to rare scores with high weight that will significantly increase the tally variance. Within MCNP, cells are 1 cm × 1 cm to provide sufficient cells to optimize over.

3. Mini2Room

The Mini2Room problem features a 0.1-MeV isotropic point source located at $(x, y) = (-15, 0)$ separated from two energy-independent 1-cm × 1-cm track-length tally regions by a shield with two streaming gaps as shown in Fig. 2. The left tally is of primary interest because it exists outside a direct streaming path; however, the right tally is also available to assess the effect of VR. In this work, all results are for the left tally. The right wall is removed to eliminate backscatter. In the MCNP calculations, continuous-energy cross sections (using MCNP's default libraries [9] for all isotopes) are used that are manually collapsed to representative multigroup scattering and absorption cross sections in COVRT. The concrete and high-density concrete use the composition from material 99 (Concrete, Regular) from [10] with the concrete at 2.3 g/cm^3 and the high-density concrete at 23 g/cm^3 (nonphysically high to create a desirable optical thickness that fits within current computational limitations). The air uses the composition and density from material 4 from [10]. It has been shown previously [7] and here that problems of this type are highly direction dependent and can cause oversplitting with automated VR techniques because of the large streaming regions.

IV. RESULTS

All of the COVRT and MCNP calculations use a high-performance workstation (64 processing cores, 528 GB RAM). The MCNP calculations use version 6.1.1b [11] and all materials use the default isotopic libraries. The COVRT and MCNP calculations use threading and all performance measures are made with consistent numbers of threads to permit fair comparisons to be made. ADVANTG calculations use MPI and are performed on a high-performance com-

puter processing node with 16 processing cores and 32 GB of RAM).

Results for Tophat & Three-Legged Duct are compared in two ways. First, the FOM for MCNP calculations with COVRT-generated VR parameters applied are compared with analog MCNP calculations where

$$\text{FOM}_{\text{CMC/MC}} \equiv \frac{\text{MCNP FOM using COVRT}}{\text{Analog MCNP FOM}}. \qquad (8)$$

Second, the mean and population variances from COVRT and MCNP are compared. As noted previously, COVRT calculates the population mean and variance (i.e., $\widetilde{D}_1$ and $\widetilde{\sigma}^2$, respectively) while MCNP directly provides the sample mean and relative error. The mean values can be compared directly but the MCNP population variance must be calculated (by computing sample variance and multiplying by the number of histories used) before being compared with COVRT. Note that when results are described, the following abbreviations are used:

- WD-WW: cell-based weight windows generated directly from a weight-dependent COVRT calculation,
- WI-I: cell-based importances generated directly from a weight-independent COVRT calculation, and
- WI-WW: cell-based importances generated from a weight-independent COVRT calculation which are manually inverted and renormalized to specify cell-based weight windows.

The WI-WW approach is used to assess the effectiveness of creating weight windows (allowing for a weight-dependent technique to be used in MCNP) based on a faster-running weight-independent COVRT calculation. Note that the difference between cell-based importances and weight windows is that the ratio of adjacent cell importances are used to unconditionally split/roulette particles and adjust the weight accordingly, whereas weight windows will only split/roulette particles (and adjust the weight) if the particle exists outside the window. Additional details are available in [9].

Mini2Room MCNP results are compared using COVRT-generated cell-based importances and ADVANTG-generated mesh-based weight windows. While this constitutes a dissimilar comparison, it represents the default mode of operation for both codes which has an effect on the FOM because of different computational burdens within MCNP. Profiling MCNP for otherwise identical calculations that have identical splitting behavior shows that mesh-based weight windows are ~22% slower than cell-based importances (with cell-based weight windows ~6% slower than cell-based importances). Note that regardless of the generating method, the cell-based importances and mesh-based weight windows are applied on the same spatial grid in MCNP for this comparison.

1. Tophat & Three-Legged Duct

For illustrative purposes, Fig. 3 shows the first and optimized second moment solutions for the Tophat calculation (recall that this is effectively an adjoint calculation). Note

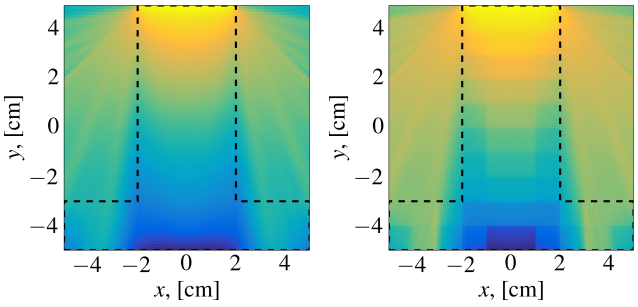

(a) M_1 (b) Optimized M_2

Figure 3: Tophat Weight-Independent COVRT Results (Tophat Outline in Dashed Lines; Color Gradient is Logarithmic Blue/Dark/Low to Yellow/Light/High)

Table I: Tophat & Three-Legged Duct FOM Ratios

Geometry	WD-WW	WI-I	WI-WW
Tophat	3.46	3.53	5.78
Three-Legged Duct	7.26	7.26	6.77

the effect of the (MCNP) cell-based weight window discontinuities and optimization mesh on M_2 in Fig. 3b. The $\text{FOM}_{\text{CMC/MC}}$ values for Tophat and Three-Legged Duct calculations are shown in Table I. In all cases, COVRT provides an improvement in MCNP FOM with the weight-independent calculations generally performing as good or better than the weight-dependent calculations. Furthermore, weight-independent COVRT calculations complete approximately an order of magnitude faster than weight-dependent counterparts (and use approximately two orders of magnitude less memory).

The ratio of the MCNP- and COVRT-calculated means and population variances are shown in Table II. From Table II, the weight-dependent Tophat and Three-Legged duct mean and variance values agree comparable to what has been observed previously. However, for the weight-independent cases the mean agrees but the variance behavior is erratic. When the COVRT angular quadrature is refined, the ratio of the mean values approach unity; however, the ratio of the variances and subsequent MCNP FOM show no substantial change. This suggests that relatively coarse quadrature is suitable to generate effective VR parameters even with an inaccurate estimate of the mean and variance. This is because of the iterative optimization that COVRT performs; relative changes in the calculation of variance (and computational time) during the perturbation process determine how VR parameters need to be adjusted rather than absolute values.

Table II: Tophat & Three-Legged Duct MCNP/COVRT Ratios For Mean & Population Variance

Parameter	WD-WW	WI-I	WI-WW
Tophat Mean	0.99	0.99	0.99
Tophat Var.	1.02	0.89	1.23
Three-Legged Duct Mean	0.77	0.77	0.77
Three-Legged Duct Var.	0.66	0.13	0.79

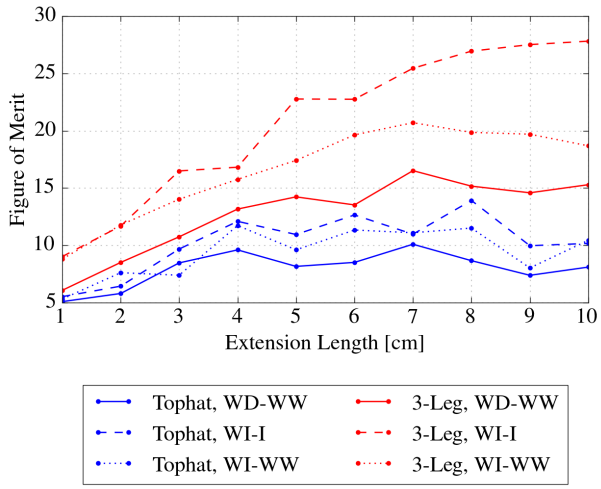

Figure 4: Tophat & Three-Legged Duct Extended Case FOM Increases vs. Analog

In addition to the geometric configurations described previously, both models are extended in the y direction between one and ten centimeters (i.e., the hat is made taller and the central leg of the duct is stretched). This was done to increase the VR difficulty of the problem. The observed FOM relative to the analog cases are shown in Fig. 4. With one exception, weight-independent COVRT calculations yield more efficient MCNP calculations than the weight-dependent calculations. As the geometry is extended, the weight-independent calculations maximize the FOM and the cell-based importances tend to perform better than the cell-based weight windows manually generated using weight-independent calculations. For both problems, there are diminishing returns on the FOM increase using COVRT because, in both cases, the problem begins to be dominated by long straight streaming.

2. Mini2Room

No fair calculation of $\text{FOM}_{\text{CMC/MC}}$ can be made because the analog case does not produce a reliable tally without an undue number of histories (by design). However, results from COVRT and ADVANTG can be compared. With ADVANTG using S_4 quadrature and 27 neutron groups, the MCNP FOM is 3.0. With weight-independent COVRT, using S_4 quadrature and 2, 4, and 8 equal lethargy neutron groups yields MCNP FOM values of 15, 6.3, and 3.8, respectively. Using the same group structure as ADVANTG, the VR parameters generated by COVRT yield an MCNP FOM of 6.5. The varying MCNP FOM values resulting from COVRT are attributed to performing multi-group COVRT calculations and then collapsing the optimized VR parameters to one-group cell-based importances (because MCNP does not support multi-group importances). A variety of collapsing schemes were explored, but no scheme gave either consistent or consistently improving MCNP FOMs. Figure 5 shows the first and optimized second moment solutions for the COVRT Mini2Room calculation. In both cases, ray effects are apparent in the vicinity of the tally region. Note that going to a higher quadrature such as S_{12} still shows pronounced ray effects for such a streaming-dominated region. In both Fig. 3 and 5, it is reasonable that the shape of M_2 follows M_1 because lower moments act as a source term for higher moments.

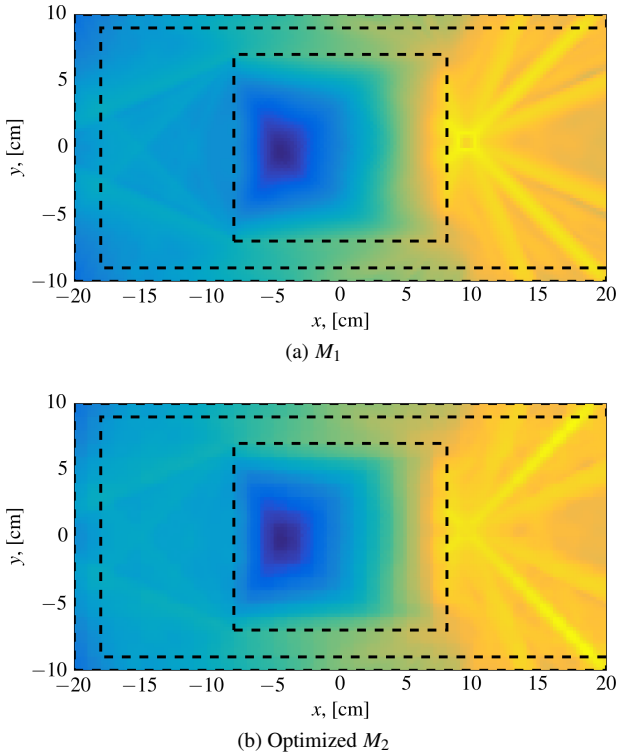

(a) M_1

(b) Optimized M_2

Figure 5: Mini2Room Weight-Independent COVRT Results (Concrete Outlines in Dashed Lines; Color Gradient is Logarithmic Blue/Dark/Low to Yellow/Light/High)

The execution time for ADVANTG is 8 seconds using 16 processors via OpenMPI while the execution times for COVRT are 0.3, 1.0, 5.3, and 48.0 hours for 2, 4, 8, and 27 groups, respectively, using 20 threads via OpenMP. The increase in time scales almost perfectly with workload (polynomial regression $R^2 = 0.9999$) because of the additional computational burden of multiple optimization passes for each energy group with minimal parallel inefficiency observed. Furthermore, it is unsurprising that COVRT takes markedly longer than ADVANTG because the method requires solving three discrete ordinates equations in an iterative optimization scheme. It is expected that additional work on the underlying sweeping algorithms would improve the performance of COVRT (a research-grade proof-of-concept code) and narrow the gap between it and ADVANTG (a production-level code). Alternatively, it would interesting to implement the multiple-moment and future time equation solves and optimizations described here into ADVANTG to see how performance is affected. However, such work would take significant effort. Finally, note that the MCNP calculation using ADVANTG-generated parameters took 3929 minutes whereas the MCNP calculations using COVRT-generated parameters took between 34–116 minutes for an equal number of histories because the COVRT parameters reduce the likelihood of long-running histories.

Because of the poor performance with both the analog and COVRT/ADVANTG-based MCNP results, and because of the highly angular nature of the problem, the problem was extended to 3D (10 cm tall with vacuum boundaries and the tallies centered axially) to test the effectiveness of incorporating a DXTRAN sphere (which cannot be used in 1D or 2D). When incorporated, the FOM for both tallies increased by a factor of 7–10. However, inclusion of DXTRAN regions is not available within COVRT and provides an area for future work.

V. CONCLUSIONS & FUTURE WORK

This summary has demonstrated the effectiveness of cost-optimized VR parameters in improving the efficiency of Monte Carlo calculations. The scale and difficulty of the problems herein have increased relative to previous comparisons. Both weight-dependent and weight-independent COVRT-generated VR parameters provide efficiency improvements to the MCNP calculations. Weight-independent COVRT calculations tend to produce more efficient VR parameters than weight-dependent calculations with the added benefit of being faster to compute. There are varying levels of agreement for the mean and variance values calculated by MCNP and COVRT; however, the FOM increase is only loosely tied to the accuracy of the COVRT calculation because the optimization process relies on relative changes. Finally, highly angle-dependent problems continue to present VR challenges when angle-independent techniques such as geometry splitting and/or weight windows are used. However, when such problems are attempted with COVRT, the benefit of cost-optimized VR parameters has been demonstrated.

Because of the execution speed advantage of cell-based importances versus either cell- or mesh-based weight windows, there may be value in revisiting multigroup importances. This is true particularly if weight-independent optimization tools such as COVRT are planned for use because of the benefits observed in all test problems. Additional work to improve the underlying sweeping algorithms of COVRT would allow a more-direct comparison with other approaches such as ADVANTG (or alternatively, directly implementing these methods in a production tool such as ADVANTG). As hybrid radiation transport methods continue to develop, it would be worthwhile to create a "standard" set of test problems used to exercise various methods on as consistent a basis as possible. Another area for future work is extending the COVRT methodology to consider DXTRAN spheres (and perhaps other shapes such as right parallelepipeds) or other variance reduction techniques to permit angular biasing. At present, no method exists to automatically specify the position and size of DXTRAN regions. Associated parameters such as the fraction of particles that initiate DXTRAN events on a cell-wise basis can also be optimized. Work to incorporate such methods into a cost-optimized procedure is currently underway.

VI. ACKNOWLEDGEMENTS

This work is supported by the Department of Energy National Nuclear Security Administration (NNSA) Engineering Campaign 7. It is also supported by the NNSA under Award Number(s) DE-NA0002576 and in part by the NNSA Office of Defense Nuclear Nonproliferation R&D through the Consortium for Nonproliferation Enabling Capabilities.

REFERENCES

1. C. J. SOLOMON, *Discrete-Ordinates Cost Optimization Of Weight-Dependent Variance Reduction Techniques For Monte Carlo Neutral Particle Transport*, Ph.D. thesis, Kansas State University (2010).
2. C. J. SOLOMON ET AL., "A Priori Deterministic Computational-Cost Optimization Of Weight-Dependent Variance-Reduction Parameters For Monte Carlo Neutral-Particle Transport," *Nuclear Science and Engineering*, **176**, *1*, 1–36 (2014).
3. S. W. MOSHER ET AL., "ADVANTG—An Automated Variance Reduction Parameter Generator," Tech. Rep. ORNL/TM-2013/416, Rev. 1, Oak Ridge National Laboratory, Oak Ridge, TN, USA (2015).
4. T. E. BOOTH and E. D. CASHWELL, "Analysis Of Error In Monte Carlo Transport Calculations," *Nuclear Science and Engineering*, **71**, 128–142 (1979).
5. N. NETHERCOTE and J. SEWARD, "Valgrind: A Framework for Heavyweight Dynamic Binary Instrumentation," in "ACM SIGPLAN 2007 Conference on Programming Language Design and Implementation (PLDI 2007)," San Diego, CA, USA (2007).
6. J. WEIDENDORFER ET AL., "A Tool Suite for Simulation Based Analysis of Memory Access Behavior," in "4th International Conference on Computational Science (ICCS 2004)," Krakow, Poland (2004).
7. J. A. KULESZA ET AL., "Application Of Automated Weight Window Generation Techniques To Modeling The Detection Of Shielded Nuclear Material," in "Advances in Nuclear Nonproliferation Technology and Policy Conference (ANTPC)," American Nuclear Society, Santa Fe, NM, USA (2016).
8. T. E. BOOTH and K. W. BURN, "Some Sample Problem Comparisons Between The DSA Cell Model And The Quasi-Deterministic Method," *Annals of Nuclear Energy*, **20**, *11*, 733–765 (1993).
9. X-5 MONTE CARLO TEAM, "MCNP — A General Monte Carlo N-Particle Transport Code, Version 5 — Volume I: Overview and Theory," Tech. Rep. LA-UR-03-1987, Los Alamos National Laboratory, Los Alamos, NM, USA (2008).
10. R. J. MCCONN JR. ET AL., "Compendium of Material Composition Data for Radiation Transport Modeling," Tech. Rep. PNNL-15870, Rev. 1, Pacific Northwest National Laboratory, Richland, WA, USA (2011).
11. T. GOORLEY, "MCNP6.1.1-beta Release Notes," Tech. Rep. LA-UR-14-24680, Los Alamos National Laboratory, Los Alamos, NM, USA (2014).